ISSN 1674-1056
http://cpb.iphy.ac.cn
http://iopscience.iop.org/cpb
中国物理 B
Chinese Physics
中国物理 Chinese Physics B

Modulation transfer spectroscopy based on acousto-optic modulator with zero frequency shift

Chen-Fei Wu(吴晨菲), Xue-Shu Yan(颜学术), Li-Xun Wei(卫立勋), Pei Ma(马沛), Jian-Hui Tu(涂建辉), Jian-Wei Zhang(张建伟), Li-Jun Wang(王力军)

Citation: Chin. Phys. B . 2018, 27(11): 114203. **doi:** 10.1088/1674-1056/27/114203
Journal homepage: http://cpb.iphy.ac.cn; http://iopscience.iop.org/cpb

What follows is a list of articles you may be interested in

Laser absorption spectroscopy for high temperature H_2O time-history measurement at 2.55 μm during oxidation of hydrogen

Yu-Dan Gou(苟于单), De-Xiang Zhang(张德翔), Yi-Jun Wang(王易君), Chang-Hua Zhang(张昌华), Ping Li(李萍), Xiang-Yuan Li(李象远)
Chin. Phys. B . 2018, 27(7): 074213. **doi:** 10.1088/1674-1056/27/7/074213

Flexible control of semiconductor laser with frequency tunable modulation transfer spectroscopy

Ning Ru(茹宁), Yu Wang(王宇), Hui-Juan Ma(马慧娟), Dong Hu(胡栋), Li Zhang(张力), Shang-Chun Fan(樊尚春)
Chin. Phys. B . 2018, 27(7): 074201. **doi:** 10.1088/1674-1056/27/7/074201

Analysis of algebraic reconstruction technique for accurate imaging of gas temperature and concentration based on tunable diode laser absorption spectroscopy

Hui-Hui Xia(夏晖晖), Rui-Feng Kan(阚瑞峰), Jian-Guo Liu(刘建国), Zhen-Yu Xu(许振宇), Ya-Bai He(何亚柏)
Chin. Phys. B . 2016, 25(6): 064205. **doi:** 10.1088/1674-1056/25/6/064205

An optical fiber spool for laser stabilization with reduced acceleration sensitivity to 10^{-12}/g

Hu Yong-Qi, Dong Jing, Huang Jun-Chao, Li Tang, Liu Liang
Chin. Phys. B . 2015, 24(10): 104213. **doi:** 10.1088/1674-1056/24/10/104213

Laser frequency stabilization and shifting by usingmodulation transfer spectroscopy

Cheng Bing, Wang Zhao-Ying, Wu Bin, Xu Ao-Peng, Wang Qi-Yu, Xu Yun-Fei, Lin Qiang
Chin. Phys. B . 2014, 23(10): 104222. **doi:** 10.1088/1674-1056/23/10/104222

Modulation transfer spectroscopy based on acousto-optic modulator with zero frequency shift*

Chen-Fei Wu(吴晨菲)[1,2], Xue-Shu Yan(颜学术)[2,3], Li-Xun Wei(卫立勋)[4], Pei Ma(马沛)[4], Jian-Hui Tu(涂建辉)[4], Jian-Wei Zhang(张建伟)[2,3,†], and Li-Jun Wang(王力军)[1,2,3,‡]

[1] *Department of Physics, Tsinghua University, Beijing* 100084, *China*
[2] *State Key Laboratory of Precision Measurement Technology and Instruments, Tsinghua University, Beijing* 100084, *China*
[3] *Department of Precision Instruments, Tsinghua University, Beijing* 100084, *China*
[4] *National Key Laboratory of Science and Technology on Vacuum Technology and Physics, Lanzhou Institute of Physics, Lanzhou* 730000, *China*

(Received 13 June 2018; revised manuscript received 31 July 2018; published online 19 October 2018)

We present a modulation transfer spectroscopy (MTS) configuration based on an acousto-optic modulator by using a variant of the typical double pass structure. One beam is modulated by using an acousto-optic modulator in opposite diffraction order to cancel the carrier frequency shift and produce a modulated pump beam. The line shape performance is investigated theoretically and experimentally. Laser frequency stabilization of the proposed configuration is demonstrated for the ^{133}Cs $|6^2S_{1/2}, F = 4\rangle \rightarrow |6^2P_{3/2}, F' = 5\rangle$ transition. The Allan deviations, which are measured by using beat note signals and the three-cornered hat method, are 3.6×10^{-11} in an integration time of 100 s and approximately 4×10^{-11} in a longer integration time.

Keywords: modulation transfer spectroscopy, laser stabilization

PACS: 42.30.Lr, 42.62.Fi, 42.60.Lh **DOI:** 10.1088/1674-1056/27/11/114203

1. Introduction

Laser frequency stabilization is widely used in atomic physics experiments and applications, such as atomic laser cooling, precision spectroscopy, and atomic clocks. A variety of laser locking schemes have been developed based on reference to an atomic transition, such as the dichroic atomic vapor laser lock[1,2] (DAVLL) and its variants[3,4] and methods based on polarization spectroscopy.[5–7] To reduce the sensitivities of a laser to fluctuations in the environmental temperature, magnetic field, and laser intensity, modulation and demodulation techniques are used to obtain dispersion spectra by using methods such as frequency modulation spectroscopy and modulation transfer spectroscopy (MTS).[8,9] The MTS is widely used in precision spectroscopy applications because of its Doppler-free background.[10]

Several MTS schemes have been reported in the literature.[11–13] The external frequency modulation required in MTS can be generated by using electro-optic modulators (EOMs),[12,14,15] acousto-optic modulators (AOMs),[16–18] or a combination of EOMs and AOMs.[13,19] Normally, a resonant circuit is used to drive an EOM, which makes it difficult to tune the modulation frequency flexibly. Comparing with the EOM, use of an AOM makes it much easier to vary the modulation frequency and implement the parameter optimization. As reported in Ref. [16], the AOMs that are used in MTS systems are often operated by using a double-pass configuration, which can result in an offset that is locked because of the doubled frequency shift. In many applications, the laser frequency is required to be stabilized based on an atomic transition. However, in the traditional MTS technique, it is necessary to use another AOM to shift the laser frequency back.

In this work, we demonstrate an alternative MTS configuration that is based on the use of a single AOM to lock the laser frequency to an atomic transition without frequency shift. The pump laser beam for the MTS passes through the AOM twice, and experiences both positive and negative first-order Bragg diffractions to cancel out the frequency shift. The radio-frequency (RF) driving signal of the AOM is modulated to generate sidebands. This AOM-based MTS system provides a convenient way to vary the modulation frequency. We investigate the MTS line shape of this configuration and its dependence on the pump beam power, the modulation frequency, and the modulation power. A laser is then frequency-locked by using this technique and the results are reported.

2. Theory

The MTS is based on four-wave mixing in a nonlinear medium. The modulation is transferred from the modulated pump laser beam to the counter propagating unmodulated probe laser beam, and thus generates the sidebands at the

*Project supported by the National Key Research and Development Program of China (Grant No. 2016YFA0302101), the Foundation of China Academy of Space Technology, and the Initiative Program of State Key Laboratory of Precision Measurement Technology and Instruments, China.
†Corresponding author. E-mail: zhangjw@tsinghua.edu.cn
‡Corresponding author. E-mail: lwan@tsinghua.edu.cn
© 2018 Chinese Physical Society and IOP Publishing Ltd

modulation frequency. The beat note signal that is observed by using a detector is in the following form:[9,14]

$$S \propto \frac{c}{\sqrt{\Gamma^2+\omega_{\rm m}^2}} \sum_{n=-\infty}^{n=\infty} J_n(\beta) J_{n-1}(\beta) \times [(L_{(n+1)/2}+L_{(n-2)/2})\cos(\omega_{\rm m} t+\varphi) + (D_{(n+1)/2}-D_{(n-2)/2})\sin(\omega_{\rm m} t+\varphi)], \quad (1)$$

with

$$L_n = \frac{\Gamma^2}{\Gamma^2+(\Delta-n\omega_{\rm m})^2}, \quad D_n = \frac{\Gamma(\Delta-n\omega_{\rm m})}{\Gamma^2+(\Delta-n\omega_{\rm m})^2},$$

where L_n and D_n describe the absorption and the dispersion, respectively, J_n is the n-th order Bessel function, β is the modulation index, $\omega_{\rm m}$ is the modulation frequency, Γ is the natural linewidth, Δ represents the frequency detuning from the line center, φ is the relative demodulation phase with respect to the modulation field that is applied to the pump laser, and constant c represents the independent parameter of the scheme. When the modulation index is lower than 1, then only the carrier and first-order sidebands are considered. Consequently, the final form of the modulation transfer line shape can be expressed as follows:

$$S \propto \frac{c}{\sqrt{\Gamma^2+\omega_{\rm m}^2}} \times J_0 J_1 [(L_1 - L_{1/2} + L_{-1/2} - L_{-1})\cos(\varphi) + (D_1 - D_{1/2} - D_{-1/2} + D_{-1})\sin(\varphi)]. \quad (2)$$

This expression contains an in-phase component (the cosine term) and a quadrature component (the sine term). The tuning of the phase of the demodulation signal enables the selection of either of the components or their combination. In addition, the sign of slope at the zero cross can also be adjusted to produce a sharp gradient without a Doppler background, which then provides an ideal error signal for laser frequency locking.

To achieve the frequency shift-free modulation, an AOM is used to build a variant of the double pass structure. The difference of this structure from the conventional structure is as follows. As shown in Fig. 1(a), the reflected laser beam does not overlap with the incident beam. The reflected beam returns along the path that has mirror symmetry with respect to the center axis in the diffraction plane. The laser beam passes through a positive first-order shift and a negative first-order shift successively, thus resulting in a zero frequency shift. Unlike the scenario of the standard double-pass system, the output beam from this configuration is spatially separated from the input beam. In addition, the reflection of the laser beam from a right-angled prism also makes it insensitive to the diffraction angle. Therefore, the AOM driving frequency can be modulated over a relatively large range and the modulated laser beam serves as a pump beam for MTS.

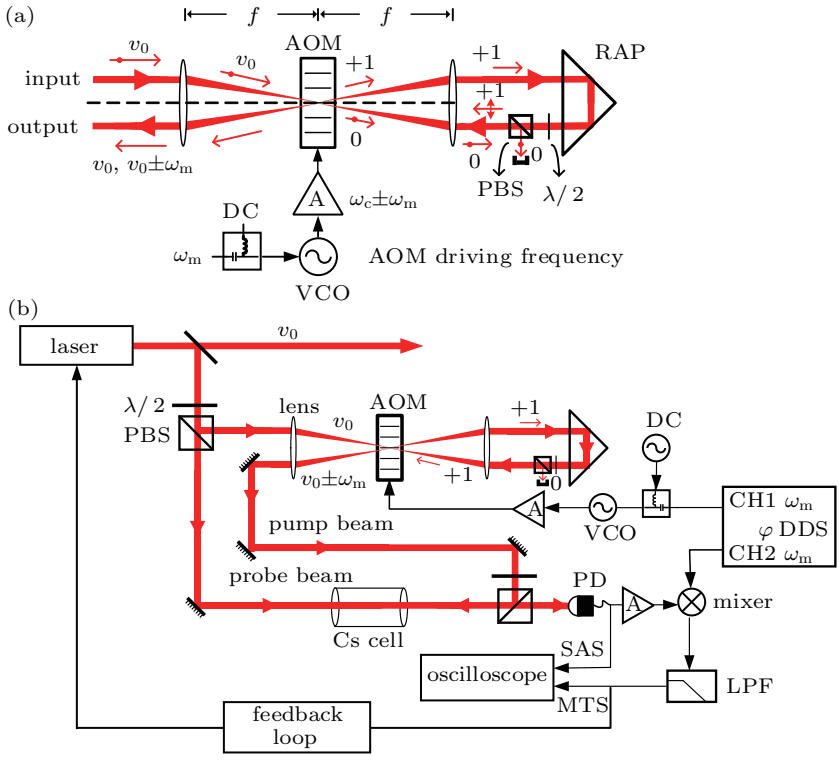


Fig. 1. (color online) (a) Schematic diagram of alternative double pass structure for frequency shift cancellation. The laser beam is focused on acousto-optic crystal; then, after positive first-order diffraction, it is collimated by using lens and reflected back symmetrically via right-angled prism; negative first-order shift then occurs in the second pass, and zero frequency shift is obtained. f: focal length of lens; AOM: acousto-optic modulator; PBS: polarizing beam splitter; $\lambda/2$: half-wave plate; RAP: right-angled prism. (b) Schematic of MTS system based on AOM with no frequency shift. A pump laser beam is modulated by using AOM and this modulation is transferred to probe beam within cesium cell. Saturation absorption spectrum (SAS) and demodulated MTS signals are monitored simultaneously on an oscilloscope. A feedback loop is used for laser frequency locking. PD: photo-detector; A: amplifier; LPF, low-pass filter.

3. Experimental setup

A schematic diagram of the experimental setup is shown in Fig. 1(b). A distributed Bragg reflector (DBR) laser operated near the D2 lines of cesium. A small fraction of the light with power of approximately 1 mW was split off for being used in MTS. This beam was subsequently divided into two parts by using a polarizing beam splitter (PBS). One beam served as a probe beam, while the other was transmitted directly into the alternative AOM double pass system to act as a pump beam and generate sidebands. The AOM (3200-124, Crystal Technology Inc.) was operated at approximately 200 MHz. The drive signal was produced by using a voltage-controlled oscillator (VCO). The frequency modulation was implemented by adding a low frequency signal $\omega_{\rm m}$ via a bias-tee. After the first pass, the zeroth-order beam and the positive first-order diffracted beam were re-collimated by using another lens. The zeroth-order beam was then blocked by using a PBS. The first-order beam was reflected by a right-angled prism (RAP) and its polarization was rotated by using a half-wave plate for transmission through the PBS, and then focused further into the AOM for the second pass. After this double pass process, the negative first-order diffraction beam from the second pass was selected as the output. In the output laser, the carrier frequency was ν_0 without a frequency shift, and the frequencies of the sidebands were offset by $\omega_{\rm m}$. To improve the diffraction efficiency of the second pass beam, the first pass beam was reflected in parallel to the incident beam and could be overlapped with the undiffracted zero-order beam by carefully adjusting the position and the angle of the RAP.

The pump beam and the probe beam were orthogonally polarized and counter propagated in the Cs cell, which was placed inside a magnetic shield and operated at room temperature. The modulation transferred from the pump beam to the probe beam via a nonlinear interaction with the atoms. The beat note of the probe beam carrier and the induced sidebands could be detected by using a fast photodiode (APD110A/M, Thorlabs). After it was amplified by using a low-phase-noise amplifier (ZFL-500LN, Mini-Circuits), the signal was then demodulated by using a mixer (ZAD-3, Mini-Circuits). The local oscillator (LO) signal was generated by using another channel of the direct digital synthesizer (DDS). The intermediate frequency (IF) output was filtered by using a homemade low-pass filter with a cutoff frequency of 8 kHz and has been used as an error signal for laser frequency locking. Finally, the error signal was transmitted to a commercial servo controller (LB1005, Newport Corporation) to generate feedback signal to the laser current.

4. Results and discussion

A typical MTS signal at a modulation frequency of 3.6 MHz is shown in Fig. 2. The saturated absorption spectrum is detected by using the same PD for comparison. In Fig. 2(a), the transition frequency of the $|6^2S_{1/2}, F = 4\rangle \rightarrow |6^2P_{3/2}, F' = 5\rangle$ transition is set to be the origin of the frequency. The beat note between the modulated pump beam and the probe beam after a negative 80 MHz frequency shift implemented by another AOM is monitored by a microwave spectrum analyzer with a span of 10 MHz, and shown in Fig. 2(b). To reduce the effect of residual amplitude modulation (RAM) on the MTS, the overlap of the pump and probe beams is adjusted to obtain a symmetric signal.[16,20,21]

The center frequency, which corresponds to 80 MHz, is the frequency difference between the carrier frequency of the pump beam and that of the shifted probe beam. The frequency differences that occur between the carrier and the two sidebands are equal to the modulation frequency, which indicates that this double pass structure imposes a fast frequency modulation on the pump beam without a carrier frequency shift; this is similar to the action of an EOM but offers more frequency modulation flexibility. Therefore, the MTS and the SAS actually correspond to the atomic transitions without a frequency offset.

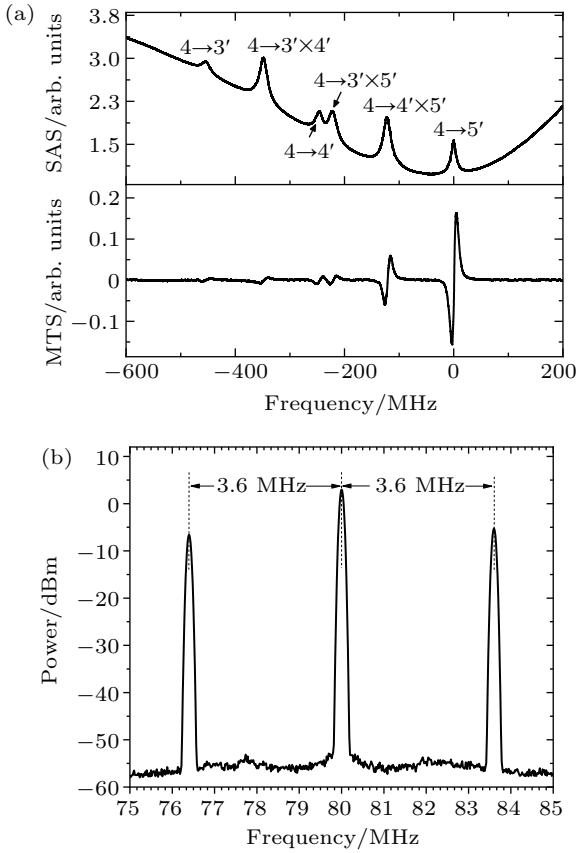


Fig. 2. (a) SAS signal and MTS signal for $|6^2S_{1/2}, F = 4\rangle \rightarrow |6^2P_{3/2}, F'\rangle$ transitions at a modulation frequency of 3.6 MHz. Zero frequency corresponds to $|6^2S_{1/2}, F = 4\rangle \rightarrow |6^2P_{3/2}, F' = 5\rangle$ cycling transition. (b) Beat note signals between the negative 80 MHz frequency shift probe beam and the modulated pump beam to monitor the pump beam frequency.

To optimize the signal and provide laser frequency sta-

bility, the peak-to-peak amplitude of the MTS signal at the cycling transition frequency is investigated for different beam powers. Because the probe intensity is much weaker than the saturation intensity, only the pump power is changed when the probe beam is maintained at 0.13 mW/cm^2.

As shown in Fig. 3, the signal amplitude increases with increasing pump beam power, and this increase stops when the cycling transition is saturated by using the pump beam power. The slope of the signal also initially increases with power and then decreases because of power broadening. Based on this result, 145 μW represents an optimal pump beam power. In the following measurements, the pump beam power is set to this value.

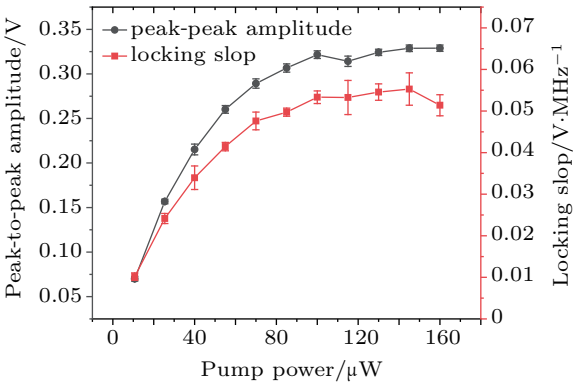


Fig. 3. (color online) Measured peak-to-peak amplitude and the locking slope caused by the change in pump beam power.

The peak-to-peak amplitudes, linewidths, and slopes of the MTS signals are investigated for different modulation signal powers and frequencies. The results are shown in Figs. 4 and 5. When the modulation frequency is set to be 3.6 MHz, the peak-to-peak amplitude of the MTS signal increases with RF modulation power increasing. For comparison with the theoretical calculations, only the $\pm 1^{st}$ order sidebands are considered, and when the power is greater than 10 dBm, the experimental results show a different growth trend. The modulation depth increases with RF power increasing, and thus the higher orders of the Bessel function must be considered. Theoretical calculations show that the linewidth of the signal's peak-peak value is independent of the power of the RF signal. However, the actual measurements show that the linewidth increases with modulation power increasing. The slope reaches a maximum value at 6 dBm before decreasing slowly with increasing power, which relates to the increase of the linewidth.

If only the modulation frequency is increased, then the modulation depth will be reduced. The measured peak-to-peak value initially increases and then decreases with as the modulation frequency increases. The measured linewidth increases with modulation frequency increasing, which is a similar result to that obtained in the theoretical calculations. The spectral line slope initially increases before decreasing. The theoretical calculations show that the maximum slope occurs at 3.6 MHz. Because the measured linewidth differs from the theoretically calculated value at 4 MHz, the spectral line slope signal reaches a maximum value at 4 MHz.

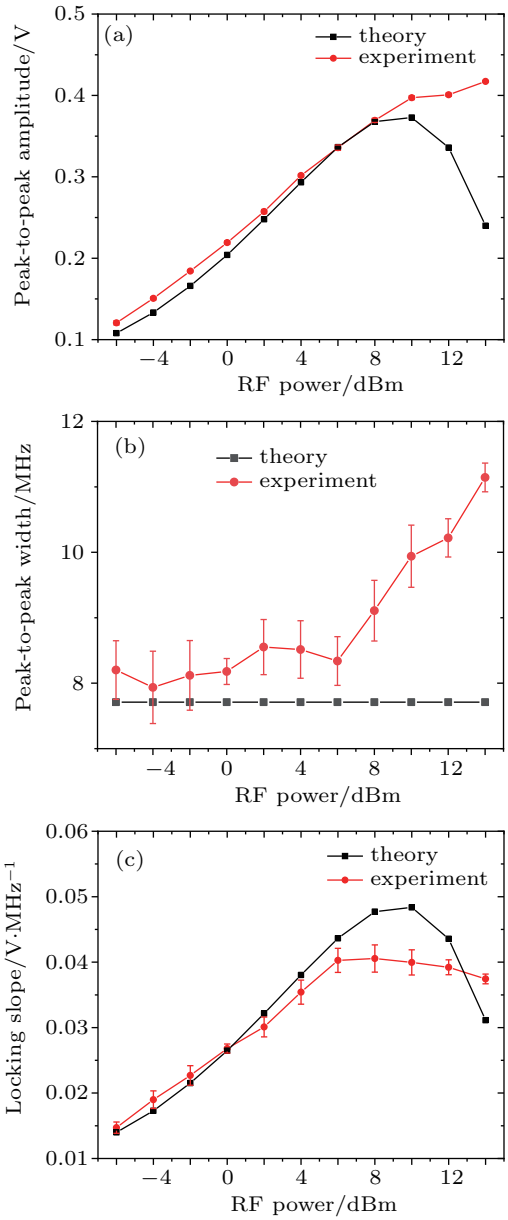


Fig. 4. (color online) Variations of MTS signal with modulation power, measured experimentally at modulation frequency 3.6 MHz: (a) peak-to-peak amplitude, (b) peak-to-peak width, and (c) locking slope.

To investigate the laser frequency locking performance of the MTS, the signal from the MTS is sent to a proportional-integral (PI) controller to lock the laser frequency to the $F = 4 \rightarrow F' = 5$ cycling transition. The laser's frequency stability is measured by using the three-cornered hat method in combination with another two laser systems that are stabilized by using the SAS technique. The beat notes are measured by using a frequency counter, which is synchronized with the same 10 MHz reference signal. The Allan deviation results for the beat note are shown in Fig. 6(a). Over the integrating

time period from 0.1 s to 1 s, the frequency stability slopes for the three laser beams show a trend of $\tau^{-1/2}$, which is mainly caused by white frequency noise. The bumps around the integrating time of 10 s in both the blue curve (MTS and laser 2) and the green curve (laser 1 and laser 2) indicate that there is a 10-s disturbance in laser 2 system, and the origin of this disturbance is not clearly determined. In the integration time of 100 s, the beat frequency stability of the MTS system with the other two reference laser systems (the black line and blue line) is worse than that between the two reference laser systems (green line), which indicates that the stability of beat notes is mainly determined by the MTS system. The resolved frequency stability of the MTS system is obtained by estimating the Allan deviation of the MTS and the corresponding deviations of the other two laser frequency locking systems while assuming that the three locking systems are all independent, which is so called three-cornered hat method. As shown in Fig. 6(b), the stability of the free-running laser is also tested for comparison by using a wavemeter (WS-U, High Finesse) at a level of 1×10^{-8} and in an averaging time of 1 s. The frequency stability of the resolved MTS system shows an improvement, with an Allan deviation of 3.6×10^{-11} over an integration time of 100 s and a level of approximately 3–4×10^{-11} for longer integration time, and is mainly dominated by the frequency flicker noise. The results for the frequency stability of the MTS signal are similar to those presented in Ref. [18].

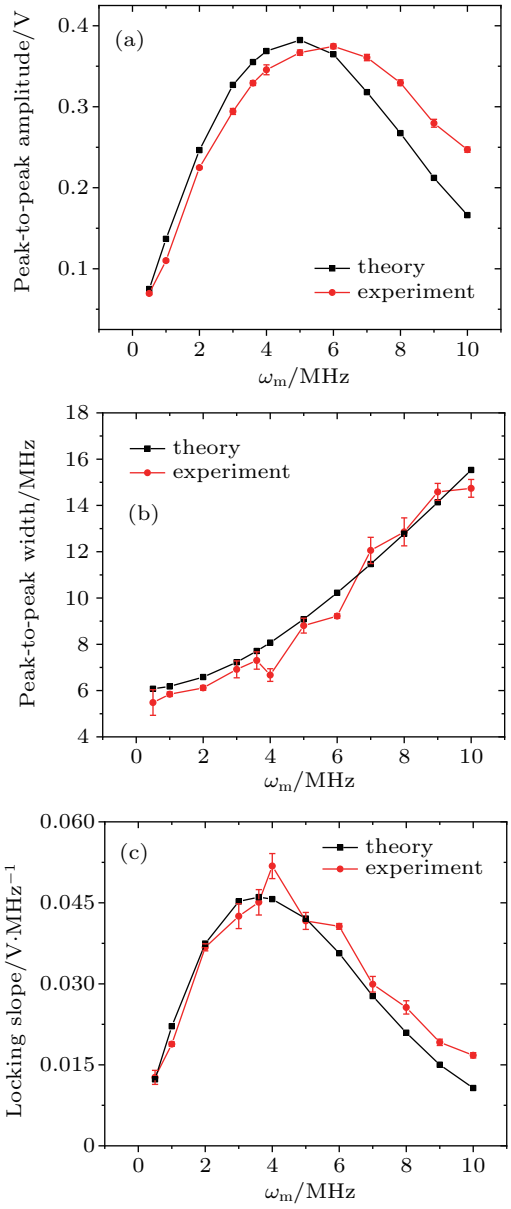


Fig. 5. (color online) Calculated and measured variations of (a) peak-to-peak amplitude, (b) peak-to-peak width, and (c) locking slope with modulation frequency at modulation power 6 dBm.

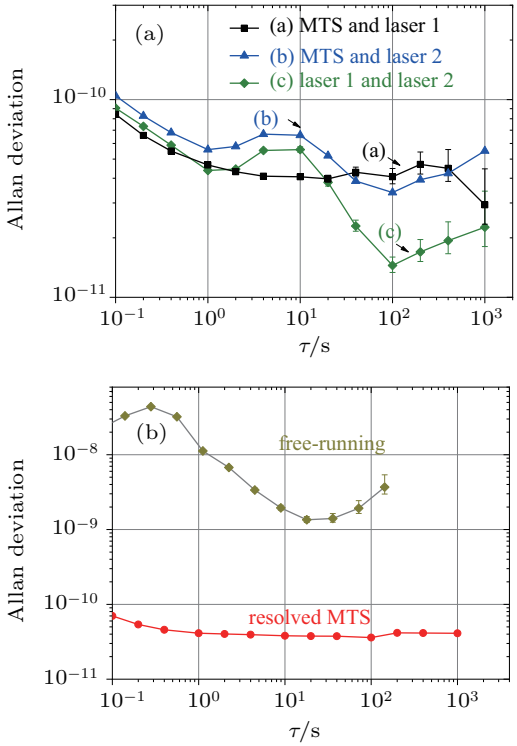


Fig. 6. (color online) (a) Allan deviations of beat frequency between the MTS signal and the signals of two other independent reference laser-stabilized systems using the saturated absorption spectrum. (b) Allan deviation of the calculated MTS estimated based on the three measurement results.

5. Conclusion

We have demonstrated a method to stabilise a DBR laser by using AOM without a carrier frequency shift in modulation transfer spectrum. The effects of the modulation frequency and power on the line shape are investigated in experiment and in numerical calculation. The frequency stability of the stabilized laser by the MTS is measured based on the three-cornered hat method through measuring the beat signals between the stabilized laser system by using the MTS and another two independently stabilized systems. The Allan deviation is evaluated to be 3.6×10^{-11} over an integration time of 100 s and reaches a level of 4×10^{-11} for longer integration time. This system may provide a useful tool for laser locking with respect to an atomic transition reference.

References

[1] Millett-Sikking A, Hughes I G, Tierney P and Cornish S L 2007 *J. Phys. B: At. Mol. Opt.* **40** 187

[2] Corwin K L, Lu Z T, H, C F, Epstein R J and Wieman C E 1998 *Appl. Opt.* **37** 3295

[3] Harris M L, Cornish S L, Tripathi A and Hughes I G 2008 *J. Phys. B: At. Mol. Opt.* **41** 085401

[4] Choi G W and Noh H R 2016 *Opt. Commun.* **367** 312

[5] Yoshikawa Y, Umeki T, Mukae T, Torii Y and Kuga T 2003 *Appl. Opt.* **42** 6645

[6] Tiwari V B, Singh S, Mishra S R, Rawat H S and Mehendale S C 2006 *Appl. Phys. B* **83** 93

[7] Torrance J S, Sparkes B M, Turner L D and Scholten R E 2016 *Opt. Express* **24** 11396

[8] Zhang Z, Wang X and Lin Q 2009 *Opt. Express* **17** 10372

[9] Shirley J H 1982 *Opt. Lett.* **7** 537

[10] Eble J F and Schmidt-Kaler F 2007 *Appl. Phys. B* **88** 563

[11] Zhang S, Zhang X, Cui J, Jiang Z, Shang H, Zhu C, Chang P, Zhang L, Tu J and Chen J 2017 *Rev. Sci. Instrum.* **88** 103106

[12] Sun D, Zhou C, Zhou L, Wang J and Zhan M 2016 *Opt. Express* **24** 10649

[13] Zi F, Wu X, Zhong W, Parker R H, Yu C, Budker S, Lu X and Muller H 2017 *Appl. Opt.* **56** 2649

[14] McCarron D J, King S A and Cornish S L 2008 *Meas. Sci. Technol.* **19** 105601

[15] Cheng B, Wang Z Y, Wu B, Xu A P, Wang Q Y, Xu Y F and Lin Q 2014 *Chin. Phys. B* **23** 104222

[16] Luo Y K, Yan S H, Jia A A, Wei C H, Li Z H, Wang E L and Yang J 2016 *Chin. Opt. Lett.* **14** 121401

[17] Negnevitsky V and Turner L D 2013 *Opt. Express* **21** 3103

[18] Zhang J, Wei D, Xie C and Peng K 2003 *Opt. Express* **11** 1338

[19] Bertinetto F, Cordiale P, Galzerano G and Bava E 2001 *IEEE T. Instrum. Meas.* **50** 490

[20] Jaatinen E and Hopper D J 2008 *Opt. Lasers Eng.* **46** 69

[21] Jaatinen E, Hopper D J and Back J 2009 *Meas. Sci. Technol.* **20** 025302